Basic Mathematics in Skin Absorption

1

Dominik Selzer, Ulrich F. Schaefer,
Claus-Michael Lehr, and Steffi Hansen

Contents

Table of Abbreviations

Symbol	Generic units	Description
A	m^2	Area of application
AUC	kg/m^3	Area under the curve
c	kg/m^3	Concentration
c_{ss}	kg/m^3	Steady-state concentration
C_0	kg/m^3	Initial concentration at $t = 0$
Cl	m^3/h	Systemic clearance
D	m^2/s	Diffusion coefficient
h_v	M	Height of applied formulation
J	$\frac{mol}{m^2 s}$	Diffusion flux
J_{max}	$\frac{mol}{m^2 s}$	Maximum diffusion flux
J_{peak}	$\frac{mol}{m^2 s}$	Peak flux
k	J/K	Boltzmann's constant
K	–	Partition coefficient
$K_{o/w}$	–	Octanol–water partition coefficient
k_p	m/s	Permeability coefficient
k_t	$\frac{\%\ applied}{s}$	Transfer coefficient
l	m	(Macroscopic) thickness
m	kg	Mass
M	kg	Mass per area
M_{ss}	kg	Steady-state amount of solute in the membrane

D. Selzer • U.F. Schaefer
Biopharmaceutics and Pharmaceutical Technology, Saarland University, Saarbrücken, Germany
e-mail: d.selzer@mx.uni-saarland.de; ufs@mx.uni-saarland.de

C.-M. Lehr • S. Hansen (✉)
Biopharmaceutics and Pharmaceutical Technology, Saarland University, Saarbrücken, Germany

Department of Drug Delivery, Helmholtz Institute for Pharmaceutical Research Saarland, Saarbrücken, Germany
e-mail: lehr@mx.uni-saarland.de; st.hansen@mx.uni-saarland.de

N. Dragicevic, H.I. Maibach (eds.), *Percutaneous Penetration Enhancers Drug Penetration Into/Through the Skin*, DOI 10.1007/978-3-662-53270-6_1

Symbol	Generic units	Description
M_∞	kg	Applied mass
MW	kg	Molecular weight
ODE	–	Ordinary differential equation
PK	–	Pharmacokinetic
r	m	Radius
S	s	Saturation concentration
t	s	Time
t_{lag}	s	Lag time
t_{peak}	s	Time to peak flux
T	K	Temperature
V	m^3	Volume
x	m	Space
η	Pa s	Viscosity
φ	$\frac{J}{mol\ K}$	Chemical potential

1.1 Mathematical Background of Analyzing Skin Absorption Processes

It is usually assumed that the travel of molecules through the skin membrane is governed simply by passive diffusion due to the absence of active transporters. From an atomistic point of view, diffusion is based on Brownian motion of particles in virtue of their thermal energy. From an empirical and more macroscopic understanding, the driving force of molecular movement is a concentration gradient of the diffusant in a medium and can be mathematically described by laws derived by Adolf Fick in 1855.

Fick's first law (Eq. 1.1) relates the diffusion flux J (e.g., in mol/m^2 s) to the concentration gradient. Here, D, the diffusion coefficient, is a proportionality constant usually given in m^2/s, and c the concentration at point x in space and time t.

$$J(x,t) = -D\ \nabla c(x,t) \tag{1.1}$$

Assuming conservation of mass, one can derive Fick's second law of diffusion (Eq. 1.2):

$$\frac{\partial c(x,t)}{\partial t} = \nabla\left(D\ \nabla c(x,t)\right) \tag{1.2}$$

In this general equation, the diffusion coefficient may vary in dependence of location and/or concentration. Additional terms can be included to address, for example, binding phenomena (Frasch et al. 2011), enzymatic reactions (Guy et al. 1987), corneocyte desquamation (Reddy et al. 2000a, b), or general convective transport to model elimination or clearance of molecules into the systematic circulation (Dancik et al. 2012). For the one-dimensional case and a homogenous medium (constant diffusivity), (Eq. 1.2) simplifies to Eq. 1.3

$$\frac{\delta c(x,t)}{\delta t} = D\frac{\delta^2 c(x,t)}{\delta x^2} \tag{1.3}$$

Homogeneity is often a strong simplification but a typical assumption for easy analytical models to describe transdermal drug transport. Solutions of these parabolic partial differential equations can be solved analytically for various initial and boundary conditions and are presented in Sect. 1.3. As mentioned earlier, these conditions often denote simplifications and are only true for the description of a specific experimental setup (e.g., infinite dose or finite dose conditions with certain initial conditions). This is a fundamental issue and must be always kept in mind when applying mathematical models in general. We will shortly discuss more flexible but complex models in Sect. 1.5 that allow the application to a wider range of scenarios.

For the inhomogeneous and more general case, the diffusion flux at a cross section x at time t is directed from sites of higher chemical potential to sites of lower chemical potential ((Eq. 1.4 (Crank 1975); Anissimov and Roberts 2004)). Inhomogenous media transitions change the classical diffusion problem to a diffusion-partition problem.

$$J(x,t) = -\frac{D}{kT}c(x,t)\frac{\delta\varphi(x,t)}{\delta x} \tag{1.4}$$

Here, $\varphi(x,t)$ is the chemical potential of the substance, T is the temperature, and k is Boltzman's constant. For the homogeneous case with $\varphi(x,t) = kT\ln(c(x,t)$ and a constant diffusivity, Eq. 1.4 simplifies to the standard diffusion equation as stated in Eq. 1.3.

The general case equation that describes the diffusion-partition problem with the chemical potential defined as $\varphi(x,t) = kT\ln\left(\left(c(x,t)/K(x)\right)\right)$, and the position-dependent partition coefficient K is given by Eq. 1.5 (Anissimov and Roberts 2004):

$$\frac{\delta c(x,t)}{\delta t} = \frac{\delta}{\delta x}\left(\begin{array}{l} D(x)\dfrac{\delta}{\delta x}c(x,t) \\ -D(x)c(x,t)\dfrac{\delta}{\delta x}\ln K(x) \end{array}\right) \quad (1.5)$$

Besides studies with variable partition and/or diffusion coefficients inside a certain skin layer (Anissimov and Roberts 2004), it is more common (especially for more complex multilayer models) to assign specific diffusion coefficients to the different layers and specific partition coefficients to the interfaces of two adjacent layers. In this chapter, the presented solutions of the diffusion equation and determination of distinctive parameters almost exclusively depend on predicted, fitted, or experimentally determined diffusivities and partition coefficients. Therefore, at least a basic understanding of the relationship between molecular properties and the aforementioned parameters is essential when it comes to the preparation, setup, and evaluation of transdermal skin transport.

For spherical particles in a continuous fluid, the diffusion coefficient can be calculated by using the well-known Stokes–Einstein relation (Eq. 1.6), with viscosity of the solvent η and particle radius r:

$$D = \frac{kT}{6\pi\eta r} \quad (1.6)$$

For diffusion in polymers, it could be found empirically that for a small particle the following relationship holds (Eq. 1.7) (Anderson and Raykar 1989):

$$D_m = D_m^0 MW^{-n} \quad (1.7)$$

Here, MW is the solute molecular weight, and n and $D_m{}^0$ are constants, the characteristics of the membrane at a specific temperature. Other theories derived from polymer research have also been applied successfully to the field of describing diffusivities in the skin domain. For deeper insight, the interested reader is kindly referred to Hansen et al. (2013).

Where the diffusivity D denotes the speed of a diffusant through a membrane and is inversely related to the weight of the solute, the partition coefficient K accounts for jumps in concentrations at the interface of two adjacent skin layers and is often related to a measure of solute lipophilicity, most commonly the logarithmic octanol–water partition coefficient. K is a thermodynamic parameter reflecting the relative affinity of a solute for a certain phase over another phase. Hence, the partition coefficient between layer m_2 and layer m_1 can be defined as Eq. 1.8

$$K_{m_2/m_1} = \frac{C_{m_2}^{\mathrm{eq}}}{C_{m_1}^{\mathrm{eq}}} \quad (1.8)$$

with $C_{m_2}^{\mathrm{eq}}$ and $C_{m_1}^{\mathrm{eq}}$ being the respective solute concentrations at the interface of the two adjacent phases at equilibrium. In general, the partition coefficient is concentration-dependent, but if the solubilities in the two phases are relatively low (which holds true for many cases), this effect can be neglected, and the partition coefficient can be defined by using the saturation concentrations S_{m_1} and S_{m_2} in the different layers (Anissimov et al. 2013), with Eq. 1.9

$$K_{m_2/m_1} = \frac{S_{m_2}}{S_{m_1}} \quad (1.9)$$

A typical strategy is to establish a relationship between an easy-to-observe parameter that mimics the membrane properties and the parameter of interest. A prominent example is the ocanol/water partition coefficient $K_{\mathrm{o/w}}$ that could be related to the stratum corneum lipid phase/water partition coefficient K_{lip}, with the help of a linear free-energy relationship (Eq. 1.10) (Anderson et al. 1988)

$$K_{\text{lip}} = aK_{o/w}^{b} \tag{1.10}$$

Here, the constants a and b correspond to the characteristics of the relationship between aqueous vehicle and lipid phase of the stratum corneum. It is obvious that this relationship strongly depends on the physicochemical properties of the layers at the interface (e.g., donor/SC or viable epidermis/stratum corneum). We again refer the interested reader to Hansen et al. (2013) for an extensive overview about the determination of diffusion model input parameters.

It must be noted that representation of diffusivity and partition coefficient in certain skin layers by a single number basically averages several transport mechanisms (e.g., several different routes through the stratum corneum or implicit binding phenomena) of the diffusant. This important fact must be kept in mind when developing and applying mathematical models as well as when trying to generalize basic relationships, such as Eqs. (1.7) and (1.10). Since literally all mathematical models heavily oversimplify the underlying physics, parameters derived from mathematical concepts might obfuscate the governing mechanics.

1.2 Analysis of Skin Permeation

Permeation experiments are usually performed to measure the amount permeated through the barrier over time in relation to the diffusion area. For an in vitro setup, this relates to the accumulated mass in an acceptor compartment. This is an important measure, especially for systemic and regional drug delivery through the skin (e.g., for achieving therapeutic drug levels systemically or treatment of tissue beneath the site of application).

Permeation experiments are typically applied using diffusion cells yielding in a general separation of the diffusion domain in different compartments, namely donor, barrier, and acceptor compartments. Frequently used diffusion cells are static cells, like the well-known vertical Franz diffusion cell (Franz 1975) and horizontal Bronaugh cell (Bronaugh and Stewart 1985) as well as flow through cells (for further details, see Sect. 3.3 of Chapter 10). Typical barrier membranes for investigation consist of excised human or animal skin in its various fashions, bioengineered skin or artificial skin surrogates (for a detailed overview, we kindly refer to Sect. 2 of Chap. 16).

When it comes to application scenarios, one can distinguish between infinite dose and finite dose experiments. In the case of infinite dosing, the applied dose is assumed to be so large that evaporation or diffusion through the barrier does only negligibly change the concentration in the donor compartment. Therefore, mathematically the dose is assumed to be infinite (Brain et al. 2002). For the finite dose case, according to the Organisation for Economic Cooperation and Development (OECD), finite dose experiments are defined by an application of a limited volume of formulation ($\leq$ 10 µl/cm^2 of a liquid formulation) (OECD 2004a, b). For semisolid and solid formulations, these values range from 1 to 10 mg/cm^2.

Typical concentration/mass/flux versus time profiles for the infinite, semi-infinite (volume > 10 µl/cm^2, but with a depletion of the donor which is already perceptive), and finite dose cases are depicted in Fig. 1.1. These theoretical calculations were performed using the DSkin® software.[1] An aqueous donor/acceptor with a drug diffusion coefficient of 6.33E-5 cm^2/s, stratum corneum lipid channel diffusion coefficient of 1.87E-8 cm^2/s, and partition coefficient of 6.56 was used for simulations. The initial donor concentration was set to 1 mg/ml, and the donor volume for the semi-infinite dose and finite dose scenario was set as 2 µl and 20 µl, respectively for an area of diffusion of 1.767 cm^2. A tortious stratum corneum lipid path length of 180 μ m was assumed, which corresponds to a swollen membrane for an in vitro setup (Talreja et al. 2001). Perfect sink conditions of the acceptor compartment are assumed.

[1] DSkin® http://www.scientific-consilience.com

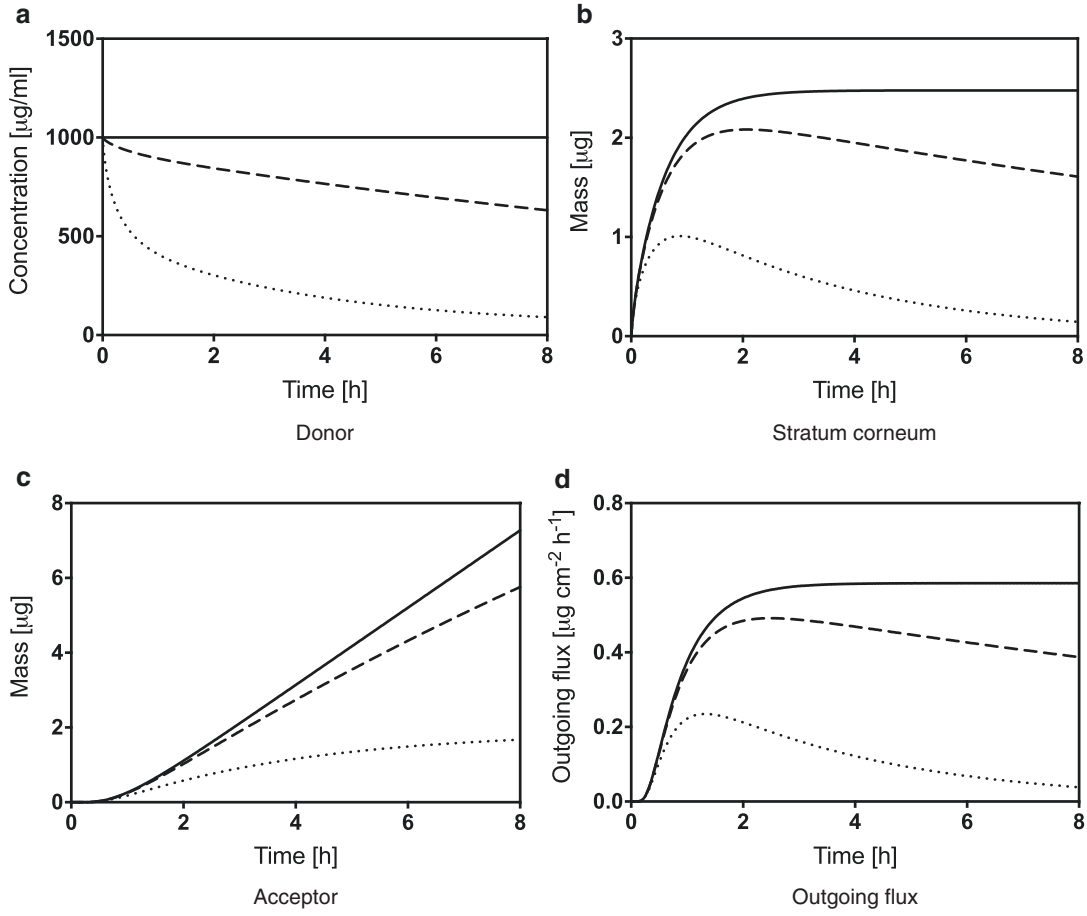

Fig. 1.1 Theoretical change of concentration in the donor compartment over time (**a**), change of mass inside the stratum corneum (**b**), accumulated mass inside the acceptor compartment (**c**), and change of stratum corneum outgoing flux (**d**) for infinite (*solid line*), semi-infinite (*dashed line*), and finite dosing (*dotted line*). Simulations were performed using the DSkin® software

The chosen values correspond to a model compound of approximately 300 Da with a $\log K_{O/W}$ of 2 in an aqueous vehicle, and model parameters were estimated by DSkin. The concentration-over-time profile depicted in Fig. 1.1a shows the characteristic depletion of the donor for the finite dose case and less pronounced for the semi-infinite case. The barrier mass-over-time curve for an infinite dose setup does reach a plateau as soon as the steady state is reached (Fig. 1.1b). As opposed to this, the mass of the finite dose case decreases after reaching a maximum (Fig. 1.1b). In case of the infinite dose setup, the accumulated mass inside the acceptor compartment reaches the typical straight steady-state line (Fig. 1.1c). This corresponds to a plateau of the flux-over-time profile (Fig. 1.1d). In contrast, the finite dose scenario will reach a theoretical mass plateau in the acceptor compartment if all substance has traveled through the membrane. Obviously, the flux reaches a maximum and subsequently decreases with time. For the simulation of the semi-infinite dose case shown in Fig. 1.1d, the applied volume per area was set slightly higher than the finite dose threshold defined by the OECD. This shows clearly that the assumption of an infinite dose (no significant depletion) does not automatically hold by applying fixed volume-based rules. This is crucial when applying the mathematical concepts presented in the next subsections, since choosing

faulty assumptions can lead to serious misinterpretation of experimental data. It has to be kept in mind that even if small volumes of highly concentrated solutions are applied and the permeation is low, the system might behave like an infinite dose case due to the fact that significant donor depletion only occurs at very long experimental time periods in relation to the permeated solute amount in the acceptor compartment.

Investigation of infinite and finite dose experiments typically differ concerning their parameters of interest and application of mathematical concepts (e.g., analytical solutions of the diffusion equation are always tailored to certain boundary and initial conditions). In the next two sections, analytical solutions of the diffusion equation and mathematical concepts for the most typical experimental settings are presented. For an exhaustive compilation of solutions regarding the diffusion equation for various boundary and initial conditions, the reader is kindly referred to the excellent book *The Mathematics of Diffusion* by J. Crank (Crank 1975).

1.2.1 Dealing with Infinite Dose Skin Permeation

Analysis of infinite dose in vitro skin permeation is typically done by measuring the cumulative amount of substance inside the acceptor compartment over time. For short times, the amount increases exponentially until reaching a steady line (the steady state) with constant flux J_{SS} (see Fig. 1.2). From a mathematical point of view, a few assumptions must be made to derive an analytical solution for the diffusion equation by defining initial and boundary conditions. In this case, we assume a constant and steady concentration in the donor compartment, perfect sink conditions (zero concentration in the acceptor at all times), and that no compound of interest is located inside the barrier at time $t = 0$.

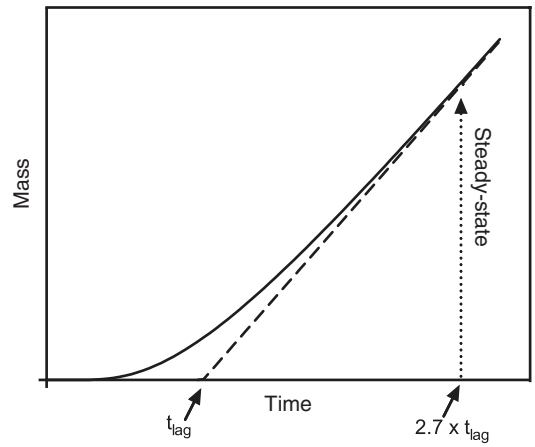

Fig. 1.2 Accumulated mass over time in the acceptor compartment of an infinite dose experiment (*solid line*) and linear part of the steady-state phase (*dashed line*). The intersection of the linearized steady-state phase and time axis denotes the lag time

By incorporating these rules for a homogeneous membrane, the absorption curve can be described by an analytical solution of Fick's second law of diffusion (Scheuplein 1967; Crank 1975), with

$$m(t) = A \times K \times l \times C_0 \left[K \times l \times t - \frac{1}{6} - \frac{2}{\pi^2} \sum_{n=1}^{\infty} \frac{(-1)^n}{n^2} \exp\left(-\frac{Dn^2 \pi^2 t}{l^2} \right) \right] \tag{1.11}$$

Here, A denotes the area of application, K is the partition coefficient between donor and barrier, C_0 is the concentration of applied formulation in the donor which is assumed not to change significantly during experimental time periods, D is the macroscopic diffusion coefficient, l is the macroscopic thickness of the barrier, and t is the time after application. It is obvious that with t leaning toward infinity (and hence reaching the steadystate), the solution simplifies to the linear part of the steady state (Fig. 1.2), with

$$m(t) = A \frac{DK}{l} C_0 \left(t - \frac{l^2}{6D} \right) \tag{1.12}$$

From Eq. 1.12, we can examine important parameters when it comes to analysis of infinite dose experiments. The first parameter is the

so-called apparent permeability coefficient, k_p, which is often given in units of cm/h and is defined as

$$k_p = \frac{DK}{l} \tag{1.13}$$

It is independent of the area of application and initial concentration, and hence a direct parameter for the strength of permeation for a compound through a certain barrier from a specific vehicle under infinite dose and perfect sink conditions. Mathematically, it denotes a normalization of steady-state flux J_{SS} with

$$k_p = \frac{J_{SS}}{C_0} \tag{1.14}$$

Such a parameter might heavily depend on experimental conditions. Hence, this has to be kept in mind when comparing parameters (interlaboratory and intralaboratory). Although k_p may be a useful and popular parameter when it comes to examination of permeation experiments, it can be sometimes misleading when comparing the permeation of several compounds (Michaels et al. 1975; Anissimov et al. 2013). The apparent permeability coefficient k_p describes an intrinsic property of a solute to permeate across a specific medium (e.g., the skin) which is independent of the dose but influenced by the applied vehicle. Therefore, comparisons are only possible between compounds which are applied in identical vehicles. In 2006, Sloan et al. introduced a change of paradigm when it comes to explaining experimental data (Sloan et al. 2006). They suggested to use the more expressive parameter J_{max} which denotes the maximum possible flux of a solute through a barrier for comparing permeability (Eq. 1.15). By using J_{max}, it is possible to overcome the limitations addressed before

$$J_{max} = k_p \times S_v = D \times \frac{S_m}{l} \tag{1.15}$$

Here, S_v is the saturated permeant concentration in the vehicle and S_m is the solubility of the solute within the barrier. In other words, by removing the influence of the partition coefficient between the skin and vehicle, J_{max} should be independent of the vehicle applied. Thus, it describes an intrinsic permeability of a solute in a certain medium, making it an ideal parameter to compare permeability of different solutes. Obviously, this is the case, as long as the vehicle does not affect the transport kinetics in the barrier (Zhang et al. 2011).

In contrast to epidermal k_p which is optimally correlated to the molecular weight and lipophilicity of a compound (Fiserova-Bergerova et al. 1990; Potts and Guy 1992; McKone and Howd 1992), Magnusson et al. (2004) could show that molecular weight is the main determinant when it comes to predicting solute maximum flux.

A further parameter to characterize infinite dose absorption is the so-called lag time t_{lag} given by

$$t_{lag} = \frac{l^2}{6D} \tag{1.16}$$

It is a measure that relates to the time it takes for a compound to travel through the barrier and establish a steady state. A word of caution is necessary concerning the meaning of t_{lag}. t_{lag} does not directly represent the time when the steady state is achieved (see Fig. 1.2); however, it can be approximated by multiplying t_{lag} with 2.7 (Crank showed that steady state is achieved when $\frac{Dt}{l^2} = 0.45$ approximately (Crank 1975)).

From a practical point of view, determination of permeability coefficient and lag time can generally be accomplished in two fashions:

1. The easiest approach utilizes the linearization of the steady state (see Fig. 1.2) which intersects the time axis at t_{lag}. This can be accomplished graphically by manual interpolation of the last data points that contribute to the steady state or mathematically more soundly by a linear fit (Schäfer-Korting et al. 2008). It is important to mention that the occurrence of physically untenable negative lag times often indicates experimental problems such as donor depletion (Barbero and Frasch 2009) or insufficient sink conditions (Anissimov and Roberts 1999). The permeability coefficient can be determined by dividing the slope of the linear part by the initial concentration C_0 and

application area A or simply by using the two steady-state data points with

$$k_p = \frac{m_{t_1} - m_{t_2}}{AC_0 (t_1 - t_2)} \tag{1.17}$$

If the slope of the curve decreases after reaching steady state, a general strategy is to employ the steepest part of the curve for evaluation (Buist et al. 2010). The clear advantage is the simplicity in calculations, but several problems arise using this approach that makes it extremely prone to errors – from an experimental and evaluation point of view:

(a) This approach cannot be applied if the steady state was not clearly reached at the end of the experiment.
(b) It is often difficult to identify which data points contribute to the steady state and which do not. Often, a frequent sampling and stepwise addition of data points from t_{end} (last data point) toward t_0 (first data point) and analyzing the linear interpolations can overcome this problem.
(c) Using only a limited amount of data points generally ignores information. Carelessly discarding data often yields wrong results and can produce a high variability, depending on which points are chosen for evaluation. This is an obvious but often neglected problem in processing experimental data.

2. A more sophisticated approach is the use of the mathematical representation of the entire curve (Eq. 1.11). In 2009, Henning et al. performed an in-depth analysis of problems that arise in data evaluation of infinite dose permeation experiments and showed the superiority of this procedure over the manual approach (Henning et al. 2009). A huge advantage is the ability to deliver sound results even if only a partial representation of the steady state is available. Often, the macroscopic thickness of the swollen skin is not exactly known. By defining partition parameter P_1 and diffusion parameter P_2 with

$$P_1 = K \cdot l \tag{1.18}$$

$$P_2 = \frac{D}{l^2} \tag{1.19}$$

and reformulating Eq. 1.11 yields (Díez-Sales et al. 1991; Kubota et al. 1993)

$$m(t) = A \cdot P_1 \cdot C_0 \cdot \left[P_2 \cdot t - \frac{1}{6} - \frac{2}{\pi^2} \sum_{n=1}^{\infty} \frac{(-1)^n}{n^2} \exp\left(-P_2 n^2 \pi^2 t\right) \right] \tag{1.20}$$

This reduces the number of unknown parameters. Hence, P_1 and P_2 can be easily fitted to experimental data using a nonlinear least squares approach. Permeability and lag time can be subsequently computed by

$$k_p = P_1 \cdot P_2 \tag{1.21}$$

$$t_{lag} = \frac{1}{6P_2} \tag{1.22}$$

1.2.2 Dealing with Finite Dose Skin Permeation

In contrast to the infinite dose exposure scenario, a typical finite dose absorption profile does not reach a steady state, but builds a mass plateau inside the acceptor compartment at late time points (see Fig. 1.1c). Finite dose experiments also show a characteristic depletion of donor concentration (Fig. 1.1a) and increase in flux until reaching the so-called peak flux J_{peak} at time t_{peak} (Fig. 1.3).

As opposed to the infinite dose case, deduction and application of an analytical solution for the description of absorption curves require a more sound mathematical foundation. Based on the theory of heat flow by Carslaw and Jaeger, a description of the flux of the compound leaving the barrier at time t is given by Eq. 1.23 (Carslaw and Jaeger 1959; Cooper and Berner 1985):

$$J(t) = 2 \cdot A \cdot M_\infty \cdot \beta \cdot \frac{D}{l^2} \sum_{i=i}^{\infty} \frac{\alpha_i^2}{\cos \alpha_i \left(\beta + \beta^2 + \alpha_i^2\right)} \exp\left(-\frac{\alpha_i^2 \mathrm{Dt}}{l^2}\right), \tag{1.23}$$

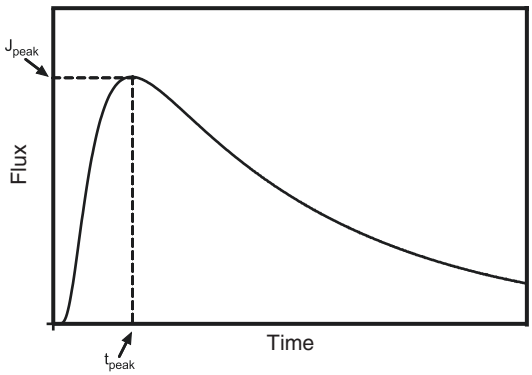

Fig. 1.3 Sketch of outgoing flux across the barrier–acceptor interface over time of a finite dose experiment (*solid line*). The maximum of the curve denotes the peak flux J_{max} at time to peak flux t_{max}

with

$$\beta = K\frac{l}{h_v}, \tag{1.24}$$

and the roots of the transcendal equation, α_i, given by

$$\alpha_i \tan\alpha_i = \beta \tag{1.25}$$

Here, M_∞ denotes the applied mass, and h_v is the height of the formulation in the donor compartment. The remaining parameters keep their meaning as introduced above.

Integrating Eq. 1.23 yields the accumulated mass per area (Kasting 2001) with

$$\frac{M(t)}{M_\infty} = 1 - 2\beta\sum_{i=i}^{\infty}\frac{1}{\cos\alpha_i\left(\beta+\beta^2+\alpha_i^2\right)}\exp\left(-\frac{\alpha_i^2 Dt}{l^2}\right) \tag{1.26}$$

In comparison to Eq. 1.11 for the infinite dose case, solving Eq. 1.26 requires a more skillful evaluation, since Eq. 1.25 must be solved for arbitrary values of i. A basic strategy to solve the transcendal equation is to use logistic regression to tabulated values of the first roots (see Fig. 1.4). To find further roots a subsequent linear extrapolation from previous roots ($\text{root}_n = 2 \times \text{root}_{n-1} - \text{root}_{n-2}$) followed by a refinement step (root-finding with, e.g., Newton's method) (Kasting 2001) is key. To reduce the number of unknowns, the same approach that worked for the infinite dose case (Eqs. 1.18 and 1.19) can be applied.

Equation 1.26 can be fitted to experimental data by a nonlinear least squares approach and yields values for β, diffusivity D, and macroscopic path length l.

Important parameters for evaluation of finite dose permeation experiments are the peak flux J_{peak} and time to peak flux t_{peak}.

A general strategy to easily find J_{peak} and t_{peak} is finding the root of the first derivative of $J(t)$ and hence solving the following equation for t_{peak}:

$$2\cdot M_\infty\cdot\beta\cdot\frac{D}{l^2}\sum_{i=i}^{\infty}\frac{\alpha_i^2}{\cos\alpha_i\left(\beta+\beta^2+\alpha_i^2\right)}\exp\left(-\frac{\alpha_i^2 Dt_{peak}}{l^2}\right)\frac{\alpha_i^2 D}{l^2} = 0 \tag{1.27}$$

A reliable solution for the root-finding problem is, for example, Brent's method (Brent 1973).

For small doses ($\beta < \sim 0.1$), J_{peak} and t_{peak} can be calculated by the following simple equations (Kasting 2001; Scheuplein and Ross 1974):

$$J_{peak} = 1.85 M_\infty\frac{D}{l^2}, \tag{1.28}$$

$$t_{peak} = \frac{\left(l^2 - h_v^2\right)}{6D} \tag{1.29}$$

If the thickness of the applied formulation is reasonably small in comparison to the macroscopic diffusion path length, it can be neglected, and Eq. 1.29 simplifies to the familiar expression:

$$t_{peak} = \frac{l^2}{6D} \tag{1.30}$$

In contrast to fitting solutions of the diffusion equation to experimental data, some researchers use the steepest linear part of the absorption curve

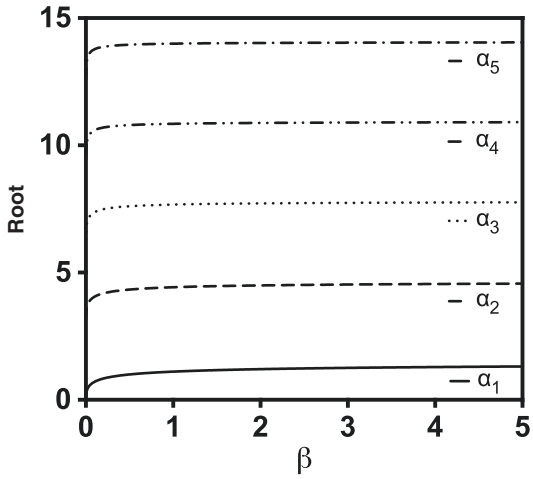

Fig. 1.4 First five roots of the transcendal Eq. 1.25 for continuous values of β from 0 to 5. Values fitted by logistic regression to tableted values from Crank (1975)

and the time to the steepest part to determine peak flux and time to peak flux (van de Sandt et al. 2004; Wilkinson et al. 2006). Obviously, as for the manual method for the infinite dose case, this approach is prone to errors. Especially for long sampling intervals, a fitting of the right kinetic representation can overcome ambiguities and imprecisions of the manual method.

For the finite dose case, finding a parameter related to the permeability coefficient is obviously not possible, since the flux changes with time. However, in 1974, Scheuplein defined the so-called transfer coefficient k_t with units of percentage of dose per time (Eq. 1.31) (Scheuplein and Ross 1974):

$$k_t = \frac{\text{flux} \times 100}{\text{specific dose}} \tag{1.31}$$

He used the early flux of the linear part of the curve to estimate the fraction of absorbed dose after a certain time by multiplying k_t by t. Besides the fact that this parameter depends on the applied dose, the amount will be heavily overestimated when the flux drops and leans toward zero. These two major drawbacks tremendously limit the usefulness of this parameter.

It has to be kept in mind that finite dose kinetics are also prone to variability of drug distribution in the donor, as shown by Hahn et al. (2012), and drug distribution to the nonincubated lateral parts in a Franz diffusion-cell setup (Selzer et al. 2013b) yielding a high variability in fitted parameters.

1.3 Analysis of Skin Penetration

1.3.1 Skin-Concentration Depth Profiles

Besides permeation profiles (accumulated mass over time) which provide valuable information about the absorption process and the transport to the blood circulation and deeper tissue, skin-concentration depth profiles supply precious data about the distribution of solute inside the barrier over time.

One of the most prominent experimental techniques to obtain skin-concentration depth profiles is tape-stripping (Stinchcomb et al. 1999; Wagner et al. 2000; Melero et al. 2011). Tape-stripping is a fast and relatively noninvasive technique to obtain absorption data for the in vitro and in vivo scenarios. For a description of the procedure, we kindly refer to Chapter 10, Sect. 3.11, and references (Escobar-Chavez et al. 2008; Lademann et al. 2009).

As for permeation experiments, the kinetics clearly differ for different exposure scenarios. Figure 1.5 shows theoretical skin-concentration depth profiles for the infinite dose case (Fig. 1.5a), semi-infinite dose case (Fig. 1.5b), and finite dose case (Fig. 1.5c). These curves were produced with the help of the DSkin software and show the change of concentration over time and space in the stratum corneum. The used input parameters correspond to the simulation parameters used to produce the permeation curves in Sect. 1.3.

The infinite dose curves show the typical exponential decay for short exposure times and transition into a straight line when steady state is reached (Fig. 1.5a). The semi-infinite case shows comparable kinetics at short times, reaches a pseudo steady state with a straight line that will drop due to the depletion of the donor over time (Fig. 1.5b). For the finite dose scenario, a straight

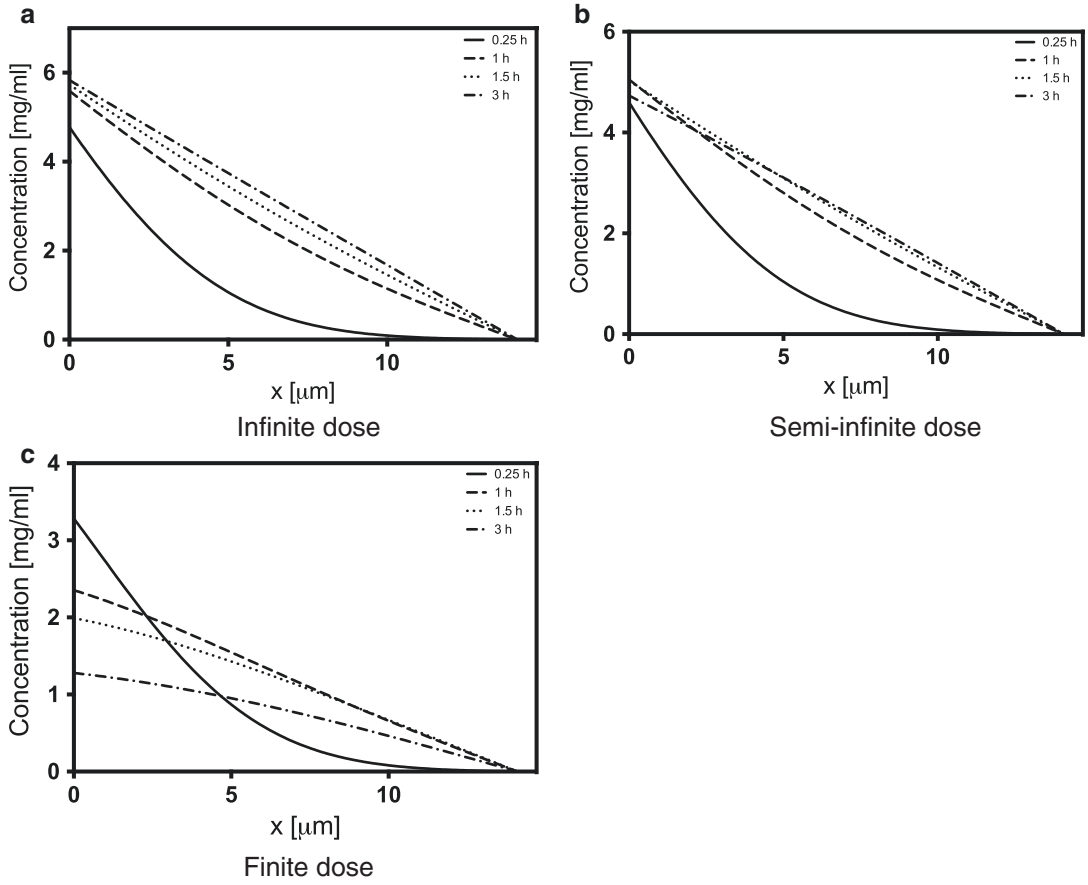

Fig. 1.5 Theoretical change of concentration in the barrier over time for the infinite dose (**a**), semi-infinite dose (**b**), and finite dose (**c**) cases. Simulations were performed using the DSkin software

line in the concentration over space kinetics is typically not reached, and a significant drop can be recognized over time (Fig. 1.5c).

As for permeation experiments, analytical solutions for the diffusion equation can be obtained to describe the change of concentration over time and space by using the appropriate initial and boundary conditions together with Eq. 1.3. For the infinite dose case, assuming a homogeneous membrane, one can calculate the concentration inside the barrier at point x and time t (Crank 1975; Hansen et al. 2008), with

$$c(x,t) = K \times C_0 \times \left(\left(1 - \frac{x}{l} \right) - \frac{2}{\pi} \sum_{n=1}^{\infty} \frac{1}{n} \sin\left(\frac{n\pi x}{l} \right) \exp\left(- \frac{Dn^2 \pi^2 t}{l^2} \right) \right) \tag{1.32}$$

As for the permeation case (Eq. 1.11), K denotes the barrier/vehicle partition coefficient, C_0 the initial concentration in the vehicle, D the apparent diffusivity, and l the macroscopic thickness of the barrier membrane with $0 \le x \le l$. The equation can only be applied if the donor does not deplete over time (typical infinite dose assumption), the receptor compartment is kept at a theoretical zero concentration (perfect sink conditions), and no solute is present inside the barrier at $t = 0$. Obviously, only the passive diffusion process is modeled. Hence, permeation

enhancement, binding phenomena, and convection effects are not part of the model.

Eq. 1.32 can be of great benefit to estimate the values for partition coefficient (K) and diffusion coefficient ($\frac{D}{l^2}$) and extrapolate the skin-concentration depth profile for later time points (Naegel et al. 2008) or even other exposure scenarios (Selzer et al. 2013a, b; Naegel et al. 2011).

For late times, the skin-concentration depth profile will reach steady state, and Eq. 1.32 simplifies to

$$c_{ss}(x) = K \times C_0 \left(1 - \frac{x}{l}\right) \tag{1.33}$$

Obviously, information about diffusivity can only be obtained before the steady state is reached. Hence, in order to obtain kinetic parameters, fitting Eq. 1.32 to experimental data should focus on short incubation times.

If experimental data that account for the depth profile at a certain time cannot be obtained immediately at the end of an experiment (e.g., due to a long tape-stripping procedure), the obtained values have to be adjusted according to the time delay (Reddy et al. 2000b), and the skin-concentration depth profile can be described with

$$c(x,t) = K \times C_0 \sum_{n=0}^{\infty} \frac{8}{(2n+1)\pi} \cos\left(\frac{(2n+1)\pi}{2}\frac{x}{l}\right) \exp\left(\frac{-(2n+1)^2 \pi^2}{24}\frac{t_d}{t_{lag}}\right) \tag{1.34}$$

Here, t_{lag} is the lag time with $t_{lag} = \frac{l^2}{6D}$, and t_d is the period of delay before the stratum corneum is stripped with $t_d = t - t_{exp}$. t_{exp} denotes the duration of exposure. Integration of Eq. 1.32 across the membrane thickness provides the area under skin-concentration depth profile curve (AUC, Eq. 1.35). The AUC equals the total amount of drug present in the membrane at time t divided by the volume of this compartment (Herkenne et al. 2006):

$$\mathrm{AUC} = K \times C_0 \left(\frac{1}{2} - \frac{4}{\pi^2} \sum_{n=0}^{\infty} \frac{1}{(2n+1)^2} \exp\left(-\frac{(2n+1)^2 \pi^2 Dt}{l^2}\right)\right) \tag{1.35}$$

In 1998, the Food and Drug Administration released a draft guidance on dermatopharmacokinetics for the evaluation of topically applied compounds (Shah et al. 1998). Besides the maximum amount in the outermost skin layer (stratum corneum) and the time to reach the maximum amount, the AUC was defined as a parameter of interest. Hence, Eq. 1.35 can be useful to predict the AUC as a function of time after obtaining K and $\frac{D}{l^2}$ from parameter fits (Herkenne et al. 2007).

For the steady state, the amount of solute in the membrane can be easily calculated from a simplified formulation of Eq. 1.35:

$$M_{ss} = A \times l \times \frac{K \times C_0}{2} \tag{1.36}$$

For the finite dose case, an analytical solution for the diffusion equation can be obtained with α and β (as defined earlier in Eqs. 1.25 and 1.24) (Kasting 2001):

$$c(x,t) = 2 \times K \times C_0 \times \sum_{n=1}^{\infty} \frac{\beta \cos(\alpha_n x/h) - \alpha_n \sin(\alpha_n x/h)}{\beta + \beta^2 + \alpha_n^2} \exp\left(-\frac{\alpha_n^2 Dt}{l^2}\right) \tag{1.37}$$

As for the infinite dose case, the same limitations hold (e.g., perfect sink conditions and no solute in the barrier at $t = 0$).

1.3.2 Skin Compartmental Approaches

Compartmental or pharmacokinetic models (PK) are used since the early beginnings of mathematical description to study the fate of a substance that was applied in the systemic circulation and are also part of the history of describing transdermal drug absorption. They treat the body as a series of well-stirred compartments. The basic idea is the elimination of space dependence of the partial differential diffusion equation (Eq. 1.2) to obtain a series of ordinary differential equations (ODEs) that describe the change of amount of solute in different compartments over time.

For the family of PK models, a set of first-order rate constant can be assigned to denote the transfer of a compound from one compartment to another. Figure 1.6 shows two examples of skin compartment models: a one-comparment skin model and a two-comparment skin model.

The corresponding first-order ODE of the one-compartment model can be expressed by Eq. 1.38:

$$V_2 \frac{\mathrm{dC}_2}{\mathrm{dt}} = k_1 C_1 - k_{-1} C_2 + k_{-2} C_3 - k_2 C_2 \quad (1.38)$$

For the two-compartment model, Eqs. 1.39 and 1.40 hold, respectively:

$$V_2 \frac{dC_2}{dt} = k_1 C_1 - k_{-1} C_2 + k_{-2} C_3 - k_2 C_2, \quad (1.39)$$

$$V_3 \frac{dC_3}{dt} = k_2 C_2 - k_{-2} C_3 + k_{-3} C_4 - k_3 C_3 \quad (1.40)$$

The separation of the skin in a lipophilic part (the stratum corneum) and hydrophilic part (viable epidermis) is common practice to mimic the heterogeneity of the skin (McCarley and Bunge 2001; Seta et al. 1992). The underlying ODEs can be solved either analytically (for the most part, only for easy equations) or numerically. Numerical solvers for nonstiff equations are, for example, Euler's method or the famous fourth-order Runge–Kutta method (widely known as RK4). For stiff equations, the backward differentiation formula (BDF) is a well-known algorithm. Commercial and free mathematical software package usually provide various possibilities for the convenient solving of these kinds of equations.

In comparison to solutions of the diffusion equation, using compartmental models can have some advantages.

A. Obviously, the solution of a set of ODEs can often be derived with little hassle in comparison to complex multicompartmental

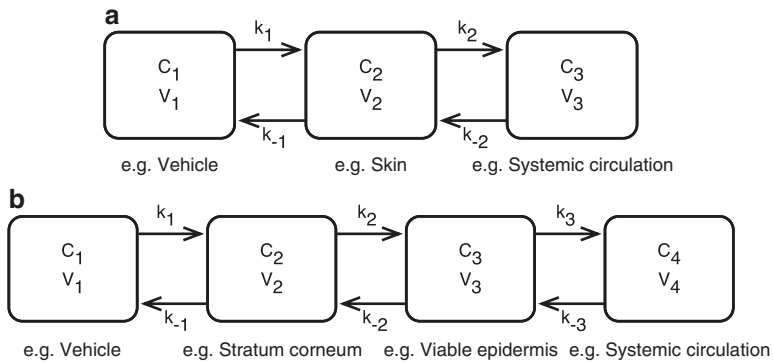

Fig. 1.6 Exemplary sketch of a one-compartment (**a**) and two-compartment (**b**) skin model. Here, the number denotes the number of compartments used to describe the skin barrier, rather than the number of overall compartments. *C* denotes the average concentration in the compartment, assuming simplified well-stirred conditions, and *V* is the volume of the compartment that is accessible for the solute distribution

diffusion models which are more cumbersome mathematically. For simple models, even analytical solutions can be derived with ease.

B. Complicated exposure scenarios with, for example, periodic application or evaporation can be implemented very easily in comparison to complex diffusion models.
C. Adding systemic PK models to a skin PK model can be achieved with little overhead.
D. Even numerical integration of the ODE is typically much faster than solving the diffusion equation numerically.

One big drawback comes with the oversimplification of having well-stirred compartments that obviously does not reflect reality. Certain kinetics, such as the transition of first-order to zero-order characteristics can only be described unsatisfactorily. PK models were typically used in the past to analyze in vivo data (Kubota 1991; Guy et al. 1982). A lot of effort was spent to relate rate constants to physicochemical parameters of the diffusant and fit experimental plasma curves or in vitro permeation profiles to PK models (Wallace and Barnett 1978; Guy and Hadgraft 1985), generally with less success than that for the class of diffusion models (Hansen et al. 2013).

Despite a growing trend toward numerical diffusion models, the class of PK models recently regained attention by the work of Davies et al. (2011). They showed that an efficient skin compartmental model can be achieved by a two-layer approach. For excellent overviews on PK models, the interested reader is kindly referred to references (McCarley and Bunge 2001; Reddy et al. 2000a; McCarley and Bunge 2000).

Besides PK models, in 1992, Seta et al. (1992) presented another compartmental approach and successfully studied the transport of radiolabeled hydrocortisone through hairless guinea-pig skin using three skin layers (stratum corneum, viable epidermis, and dermis). They divided each compartment into several hypothetical thin elements and calculated the flux between each element. This approach can be numbered among compartmental models, but rather trends toward numerical finite difference approaches which we will present briefly in Sect. 1.5.

1.4 Advanced Mathematical Approaches for Studying Skin Absorption

Previously, we presented basic mathematical concepts to analyze skin permeation and penetration experiments. These models typically relied on analytical solutions of the diffusion equation in the time and/or space domain (see Sects. 1.3 and 1.4.1) or used simple compartmental simplifications to represent the skin (see Sect. 1.4.2). In this section, we will briefly discuss more advanced models that are capable of describing more complex exposure scenarios on a macroscopic and microscopic scale. Statistical models (such as QSAR models (Potts and Guy 1992; Wilschut et al. 1995) or statistical learning approaches (Neumann et al. 2005; Agatonovic-Kustrin et al. 2001; Chen et al. 2007)) that are typically restricted to making predictions are beyond the scope of this chapter. The interested reader is referred to references (Patel et al. 2002; Fitzpatrick et al. 2004; Neumann 2008)

1.4.1 Laplace Domain Solutions

Another popular approach to solve the diffusion equation for various scenarios is the application of the Laplace transform to an objective function (Hadgraft 1979, 1980; Guy and Hadgraft 1982). Generically, for a concentration function $C(x,t)$, the Laplace transform L is defined as

$$\hat{C}(x,s) = L\left(C(x,t)\right) = \int_0^\infty C(x,t)\exp(-st)\,dt \tag{1.41}$$

The huge advantage of solving partial differential equations (PDE) with the help of Laplace transforms is the reduction of a PDE to an ordinary differential equation (ODE) which can be solved much more easily. In comparison to analytical solutions in the time domain, Laplace solutions of the diffusion equation typically lack infinite sums and can be expressed for various exposure conditions with relatively simple adaptions. A drawback is the need of (numerical) inversion to the time domain, but most mathematical or

scientific software packages are capable of performing this task easily and in a convenient manner. Some important parameters, such as steady-state flux and lag time can even be extracted from the Laplace solution without inversion (Anissimov and Roberts 1999).

Solutions for special cases of variable partition and/or diffusion coefficients inside the stratum corneum are available in the Laplace space (Anissimov and Roberts 2004). Finite dosing and finite receptor and variable receptor clearance for the infinite dose scenario could be successfully modeled by Anissimov and Roberts (1999, 2001). Frasch fruitfully applied a Laplace domain solution from Anissimov and Roberts to simulate the permeation of theophylline through the stratum corneum incorporating slow binding phenomena (Anissimov and Roberts 2009; Frasch et al. 2011). Even the effect of desquamation could be investigated, and Simon et al. delivered Laplace domain solutions for different epidermal turnover rates (Simon and Goyal 2009).

For further reading, Anissimov et al. compiled a large amount of Laplace domain solutions of the diffusion equation for different scenarios in reference (Anissimov et al. 2013).

1.4.2 Numerical Diffusion Models

Numerical methods for solving the diffusion equation for various initial and boundary conditions are important techniques and allow a more flexible construction of advanced skin models (e.g., incorporation of binding effects (George 2005)), iontophoretic transdermal delivery (Wearley et al. 1990), repeated applications (Kubota et al. 2002), controlled release vehicles (Kurnik and Potts (1997), and in vitro lateral transport (Selzer et al. 2013a, b)). In comparison with classical PK skin compartment models, it is typically much more convenient to relate the necessary input parameters (for the simple diffusion problem, only diffusivities and partition coefficients are needed) to physicochemical parameters of the diffusant (Hansen et al. 2013). These models can be used for descriptive and predictive tasks as well as for the theoretical investigation of the interplay among input parameters. The basic idea consists of the discretization of time and space domain (gridding) and a numerical approximation of the partial differential diffusion equation (e.g., for the most trivial form, see Eq. 1.2). The discretization allows the construction of coarse-grained macroscopic and fine-grained microscopic models (a basic example is depicted in Fig. 1.7).

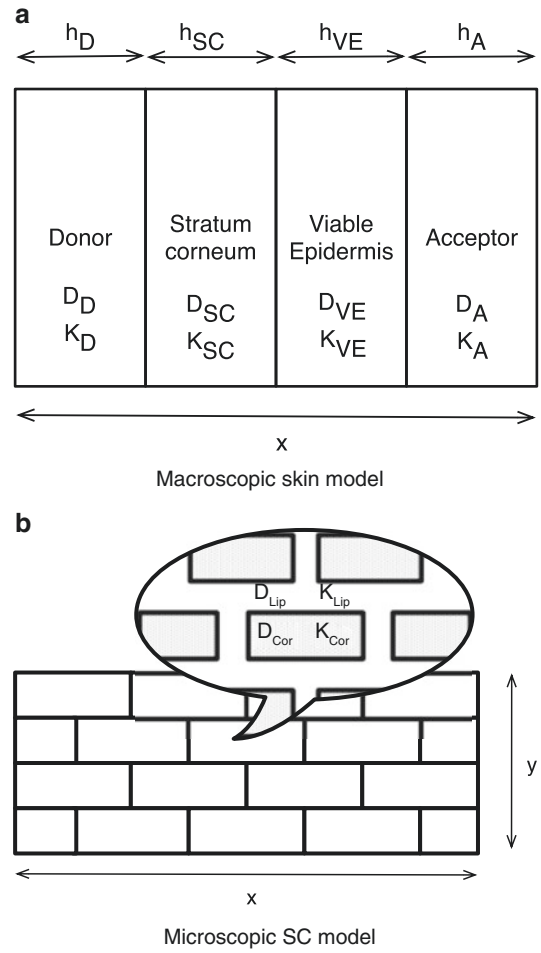

Fig. 1.7 Simplified depiction of a macroscopic diffusion model with effective diffusivities and partition coefficients (**a**), and a microscopic representation of the brick-and-mortar structure (Elias 1983) of the stratum corneum (SC) with diffusivities and partition parameters for the lipid and the corneocyte phase (**b**). Figures are not drawn to scale

Macroscopic models do neglect the heterogeneity of different skin layers and use effective kinetic parameters of a diffusant for each layer to

describe the transport process. Usually, these kinds of models are only needed for solving the underlying diffusion equation for the one-dimensional case and hence treat the skin as a series of multilayered slabs (Fig. 1.7a).

Microscopic models allow a heterogeneous representation of the stratum corneum (Hansen et al. 2009) (lipid phase and protein phase, see Fig. 1.7b) and hence yield a more in-depth analysis of the underlying transport processes. In this case, the absorption kinetics do not only rely on the definition of diffusion parameters but also on the definition of spatial geometry. Due to the high spatial resolution, these models typically require much higher computational costs in comparison to coarse-grained macroscopic models. By mathematical homogenization, it is possible to reduce a microscopic model to a macroscopic one with preservation of model properties (e.g., anisotropic diffusivity in the stratum corneum) (Muha et al. 2010; Selzer et al. 2013b).

From a numerical perspective, several techniques exist to approximate the solution of the diffusion equation. For the one-dimensional case, probably the most prominent method is the finite differences approach. Assuming a constant diffusivity, Eq. 1.2 can be approximated by

$$\frac{C_i^{t+1} - C_i^t}{\Delta t} = D \frac{C_{i-1}^t - 2C_i^t + C_{i+1}^t}{(\Delta x)^2} \tag{1.42}$$

The left-hand side of equation is approximated by first-order forward differences and the right-hand side by second-order central differences that both arise from Taylor series expansions. As for every numerical method, the time and space domain is discretized. In this case, C_i^t denotes the concentration at point $i \times \Delta x$ for time $t \times \Delta t$, with a system of constant space step size Δx and time step size Δt. Obviously, the above-mentioned equation can be easily generalized to problems in 2D and 3D space. Reformulation of Eq. 1.42 yields

$$C_i^{t+1} = MC_{i-1}^t + (1-2M)C_i^t + MC_{i+1}^t \tag{1.43}$$

with

$$M = D \frac{\Delta t}{(\Delta x)^2} \tag{1.44}$$

Because of the fact that every point of a certain layer only depends on points from the past, there is no functional relationship between different points of one time layer (it is a so-called *uncoupled problem*). This leads to the problem of numerical instabilities that depend on the value of M (Eq. 1.44) and hence on the choice of Δt for a given spatial resolution Δx. It can be shown that this explicit method is only stable for values of $M \leq 0.5$ (for the one-dimensional case). A violation of this recommendation can produce noise which may result (empirically, it always does for the diffusion equation) in nonsmoothable rounding errors. For small diffusion coefficients (e.g., in the stratum corneum), this restriction can lead to extremely small time steps and therefore to high computational runtimes.

An elegant way to overcome this problem is by the use of implicit methods that rely not only on data from the last time point. Undoubtful, the most widely used approach is the so-called Crank-Nicolson method (Crank 1975) (Eq. 1.45) that is unconditionally stable and provides a better overall error than the explicit approach:

$$\frac{C_i^{t+1} - C_i^t}{\Delta t} = \frac{D}{2}\left(\frac{C_{i-1}^{t+1} - 2C_i^{t+1} + C_{i+1}^{t+1}}{(\Delta x)^2} + \frac{C_{i-1}^t - 2C_i^t + C_{i+1}^t}{(\Delta x)^2} \right) \tag{1.45}$$

This equation yields a system of linear equations (tridiagonal matrix) that can be efficiently solved by, for example, the Thomas algorithm (an optimized form of Gaussian elimination that can solve tridiagonal systems of equations). Using this implicit method, it is possible to choose larger time steps, which decrease the number of computational steps in spite of the

fact that the solving of the system of linear equations is computationally more complex compared to the explicit method. Various works on modeling transdermal transport that are based on finite differences exist (Kurnik and Potts 1997; Kubota et al. 2002; George 2005; Nitsche and Frasch 2011).

Finite differences are not the only mesh-based technique to find approximate solutions to partial differential equations, as the diffusion equations. The method of finite elements that is widely used in the field of mechanical engineering and finite volume approaches that can efficiently handle unstructured girds and is often applied in the field of computational fluid dynamics are known to successfully model transdermal transport (Barbero and Frasch 2005; Heisig et al. 1996; Naegel et al. 2008, 2011; Selzer et al. 2013b). For excellent overviews about numerical models, the interested reader is kindly referred to references (Frasch and Barbero 2013; Naegel et al. 2013).

1.5 In Vitro–In Vivo Correlation (IVIVC)

In vitro–in vivo correlations (IVIVC) address the question of the significance of in vitro data for predicting the situation in the living being. In vitro data are often compared to in vivo data from studies obtained under different experimental circumstances, and exact information on relevant experimental conditions is frequently lacking (ECETOC 1993). Factors which are known to influence transdermal absorption include among others the exposure conditions (such as dose, vehicle, humidity, temperature, and exposure duration), the skin type, and anatomical site of application (for more information, the interested reader is referred to Chapter 10 in this book). Therefore, only data which were obtained using harmonized protocols should be compared. The type of data obtained in in vitro and in vivo studies is usually quite different mostly due to experimental, physiological, and ethical constraints. Several different endpoints can be used to relate in vitro to in vivo skin absorption data. This paragraph should give an overview on which kind of data can be used for the purpose of establishing IVIVC.

The topic of IVIVC is especially relevant for estimating bioavailability (BA) and for bioequivalence (BE) testing of topically applied dosage forms. For systemically acting drugs, BE is generally demonstrated based on a pharmacokinetic study comparing the plasma levels of test and reference product, following the idea that the pharmacokinetics are correlated to the pharmacological effect. Similarly, it is possible for transdermal patches which act systemically to demonstrate BE based on plasma levels or excretion data. In particular, a transdermal patch provides an infinite source and controls the invasion rate into the blood similar to an i.v. infusion. Consequently, in this case, the transdermal absorption rates which are measured in vitro can be correlated with the plasma concentrations (Chien et al. 1989; Franz et al. 2009).

Finite dosing is of course more relevant to the real exposure to chemicals or actives, and consequently also for demonstrating IVIVC (Bronaugh and Maibach 1985). At the same time, accurately detecting the low systemically absorbed and excreted amounts of solutes which are applied to the skin as a finite dose requires sensitive and selective analysis in complex biological media (blood, urine). Data which were obtained during the 1960s–1980s therefore often report radioactivity labeling as a technique to obtain pharmacokinetic data, for example, form excretion to the urine in human volunteers (Feldmann and Maibach 1969; Bartek et al. 1972; Feldmann and Maibach 1974; Wester and Maibach 1976). Indeed, if skin penetration is the rate-limiting step, the rate at which the compound appears in the urine will represent the rate at which it penetrates the skin. For solutes which are also fecally excreted, a correction for the proportion of urinary to fecal excretion is required. Results are calculated as percent of the applied doses which are excreted over time and corrected for application area and incomplete urinary excretion; division by time gives the absorption rate (Feldmann and Maibach 1969, 1974).

Likewise, if one assumes that the steady-state flux through skin in vitro (J_{ss} [μ g/cm^2/h]) is

equivalent to the rate of input to the systemic circulation in vivo, then in vitro percutaneous absorption data can be used, for example, during formulation development for formulation optimization based on known clinical data:

$$J_{ss} \times A = C_{ss} \times Cl \tag{1.46}$$

Here, A [cm^2] = area of skin, C_{ss} [μ g/l] = steady-state blood concentration, and Cl [l/h] = systemic clearance. With C_{ss} and Cl being known, for example, from i.v. application, a target flux can be calculated which needs to be achieved with a developed dosage form to obtain plasma levels accordingly (Franz et al. 2009).

Cnubben et al. further used linear systems dynamics (Opdam 1991; Vaughan and Dennis 1978; Fisher et al. 1985) to calculate an in vivo percutaneous absorption rate (μ g $cm^{-2}h^{-1}$) based on the plasma concentration–time profile of solutes after dermal application and after a reference i.v. administration (Cnubben et al. 2002). From this, they derived in vivo permeability coefficients and lag times and compared these to values obtained in vitro.

Difficulties arise for topically (i.e., on or in the skin) or regionally (i.e., in nearby tissues, such as the joints, muscle, or cartilage) acting drugs for which the plasma concentration is neither quantifiable nor relevant for their local activity. For those drugs, measuring the drug concentration at the site of action, or dermatopharmacokinetics (DPK), will be more relevant. Unfortunately, a draft guidance document recommending tape-stripping for demonstrating BE of topically acting drugs was withdrawn in 2002, due to issues arising from poorly defined experimental standardization. Currently, tape-stripping is only recommended by the FDA for BE testing for certain classes of drugs, such as for antifungals that target the stratum corneum itself (Narkar 2010). This results in the unfortunate situation that the in vivo skin blanching or vasoconstriction assay (only for corticosteroids) is currently the only FDA-recommended assay for demonstrating BE of generics which does not rely on clinical studies (with known problems such as poor sensitivity, requirement for high number of test persons, and consequently high costs). Franz et al. have collected substantial evidence that in vitro skin absorption testing may be used as a surrogate method for in vivo BA or BE testing (Franz et al. 2009). In particular, two types of measurements are being discussed for this purpose. First, these are the already mentioned tape-stripping DPK measurements which can be performed in vivo as well as in vitro (for more details, the interested reader is referred to references (Herkenne et al. 2008; Russell and Guy 2009)). Second, these are also permeability measurements which are performed in vitro.

In fact, Franz et al. reported that the in vitro method was able to discriminate between different vehicles, a finding which was also supported by differences in clinical efficacy, while this difference was not picked up by the vasoconstriction assay (Franz et al. 2009). Importantly, Franz et al. as well as others demonstrated excellent IVIVIC, provided that the study protocols between in vitro and in vivo studies were harmonized (Franz et al. 2009; Lehman et al. 2011). The latter aspect is certainly very important to ensure comparability between in vitro and in vivo results. Treffel and Gabard as well as Chatelain et al., later in a follow-up study, noticed that differences between several sun protection products which were obvious in tape-stripping experiments as well as sun protection factor (SPF) measurements in human volunteers as early as 30 min after application could in vitro not be detected until later time points, that is, 6 h (Treffel and Gabard 1996; Chatelain et al. 2003). In vivo and in vitro protocols differed in terms of the applied dose (2 mg/cm^2 vs. 3 mg/cm^2). The differences may be also explained by artifacts from nonphysiological swelling of the skin inside the Franz diffusion cell obscuring early effects.

Comparing the skin penetration of the nonsteroidal anti-inflammatory drug flufenamic acid in vitro and in vivo by tape-stripping, Wagner et al. observed that the in vivo levels were consistently lower than the in vitro levels which they found inside the stratum corneum after different incubation times (Wagner et al. 2000). The reasons for these differences can be manifold, such as interindividual differences, regional variances, different pressures applied during tape-stripping

to name but a few. Nonetheless, correlating the amounts found after different incubation times, they demonstrated an excellent IVIVC (Wagner et al. 2000). To exclude interindividual differences in a follow-up study, Wagner et al. designed a special workflow, where they used abdominal skin from the same exact individual before and after undergoing abdominal reduction surgery (Wagner et al. 2002). Unfortunately, the results obtained from tape-stripping were not usable due to the disinfectant wipe which was necessary for the surgery and which significantly changed the drug levels inside the upper skin layers. However, they could show excellent agreement of the drug levels inside the deeper skin layers (Wagner et al. 2002). This collection of reports shows that obtaining a good IVIVC is possible. However, the parameters which should be correlated need to be carefully selected, and the conditions under which these parameters are obtained are most critical.

1.6 Tips and Tricks

This section supplies information about common difficulties when computing analytical solutions of the diffusion equation and fitting these solutions to experimental data. It should work as a guide when conducting mathematical analysis of experimental data.

1.6.1 Infinite Sums in Analytical Solutions

Many analytical solutions presented in this chapter include an infinite sum of form

$$F(x) = a\sum_{i}^{\infty} H_i(x) + b, \qquad (1.47)$$

with $H_i(x)$ going to zero for i going to infinity. These are typical examples of solutions of the diffusion equation for various scenarios. Being able to deal with this kind of equations is a key requirement for a sound evaluation of skin transport experiments. Hence, we will give a few hints for the solid handling.

From a practical point of view, the infinite sum has to be truncated at some point. Some researchers only use <10 summations, for example, for the infinite dose solution presented in Sect. 1.3.1, since the subsequent terms do not significantly contribute to the overall result (Frasch and Barbero 2008). To achieve maximal accuracy, a more precise way to truncate the sum is to incorporate a relative threshold, like the so-called machine epsilon of the computer – a relative error due to rounding in floating point arithmetic (Hansen et al. 2008). The machine epsilon ε_0 is defined as the smallest number, such that $1+\varepsilon_0 > 1$ holds for a certain machine.

Nowadays, implementing more complex functions and fitting to experimental data can be achieved easily using commercial or free data analysis and statistical software packages or free scripting languages. For example, the authors used the popular scripting language *Python*[2] in combination with the *SciPy* package (scientific python) (Jones et al. 2001) to compute various equations presented for the finite dose case. These kinds of packages provide predefined functionalities for root-finding, fitting, and plotting.

1.6.2 Fitting of Experimental Data

As reported here, fitting of experimental data to analytical solutions of the diffusion equation is an excellent way of analysis. To gain confidence, experiments are typically conducted in a recurrent manner. For data evaluation, researchers can fit the objective function to either each individual dataset (of every single experiment) or a combination of experimental data (e.g., mean accumulated mass over time).

It is strongly recommended to report the evaluation of single experiments (OECD 2004b), and the authors support the approach of individual evaluation of experiments and averaging of individual determined parameters. Despite this fact, many researchers prefer to handle arithmetic means of combined experiments (Schäfer-

[2]Python: http://www.python.org

Korting et al. 2008). Fitting is typically done by applying a linear or nonlinear least-squares approach. The basic idea is to minimize the sum of squared residual errors (e.g., minimization of the so-called weighted root mean square function displayed in Eq. 1.48):

$$\mathrm{RMS} = \sqrt{\frac{1}{n}\sum_{i=1}^{n} w_i \left(d_i^{\exp} - d_i^{\mathrm{calc}}\right)} \qquad (1.48)$$

Here, n is the number of data points, $d_i^{\exp}$ is the ith data point, d_i^{calc} is the quantity that is being modeled (e.g., concentration in the membrane at time t and point x or cumulative amount of substance in the acceptor compartment), and w_i are optional weights for every d_i pair. These weights are capable of emphasizing or de-emphasizing certain data points. If no weighting is applied, w_i is 1 for every i.

To emphasize experimental uncertainties, a typical choice of weights is $w_i = \frac{1}{\sigma^2}$ (Henning et al. 2009). This requires knowledge about the kind of underlying error or variation. Using the standard deviation is not the only option to weight data. Krüse et al. suggested a weighting scheme with $w_i = \frac{1}{|t_i|}$ to de-emphasize later time points (Krüse et al. 2007). This can be helpful for example, for fitting accumulated mass versus time data for the infinite dose case, since it is well known that the standard errors of later time points are additive in nature (Selzer et al. 2013a).

Fitting finite dose permeation data can be prone to variabilities in the unknowns (especially the partition coefficient). A stabilization can be achieved by either fixing an unknown to a constant value and/or fit data from several doses at once (Kasting 2001).

Conclusion

We hold powerful mathematical tools in our hands which allow us to interpret experimental data, predict relevant endpoints, and improve our understanding of skin absorption. They find their applications in various fields, including toxicology, drug delivery, or regulatory affairs. Key to the useful application of such mathematical tools is a fundamental understanding of the underlying physical and biological mechanistics but also of experimental and model constraints. These were highlighted in this chapter.

References

Agatonovic-Kustrin S, Beresford R, Yusof APM (2001) ANN modeling of the penetration across a polydimethylsiloxane membrane from theoretically derived molecular descriptors. J Pharm Biomed Anal 26(2): 241–254

Anderson BD, Raykar PV (1989) Solute structure–permeability relationships in human stratum corneum. J Invest Dermatol 93(2):280–286

Anderson BD, Higuchi WI, Raykar PV (1988) Heterogeneity effects on permeability–partition coefficient relationships in human stratum corneum. Pharm Res 5(9):566–573

Anissimov YG, Roberts MS (1999) Diffusion modeling of percutaneous absorption kinetics. 1. Effects of flow rate, receptor sampling rate, and viable epidermal resistance for a constant donor concentration. J Pharm Sci 88(11):1201–1209

Anissimov YG, Roberts MS (2001) Diffusion modeling of percutaneous absorption kinetics: 2. Finite vehicle volume and solvent deposited solids. J Pharm Sci 90(4):504–520

Anissimov YG, Roberts MS (2004) Diffusion modeling of percutaneous absorption kinetics: 3. Variable diffusion and partition coefficients, consequences for stratum corneum depth profiles and desorption kinetics. J Pharm Sci 93(2):470–487

Anissimov YG, Roberts MS (2009) Diffusion modelling of percutaneous absorption kinetics: 4. Effects of a slow equilibration process within stratum corneum on absorption and desorption kinetics. J Pharm Sci 98(2):772–781

Anissimov YG, Jepps OG, Dancik Y, Roberts MS (2013) Mathematical and pharmacokinetic modelling of epidermal and dermal transport processes. Adv Drug Deliv Rev 65(2):169–190

Barbero AM, Frasch F (2009) Pig and guinea pig skin as surrogates for human in vitro penetration studies: a quantitative review. Toxicol In Vitro 23(1):1–13

Barbero AM, Frasch HF (2005) Modeling of diffusion with partitioning in stratum corneum using a finite element model. Ann Biomed Eng 33(9):1281–1292

Bartek MJ, LaBudde JA, Maibach HI (1972) Skin permeability in vivo: comparison in rat, rabbit, pig and man. J Invest Dermatol 58(3):114–123

Brain KR, Walters KA, Watkinson AC (2002) Methods for studying percutaneous absorption. In: Walters KA (ed) Dermatological and transdermal formulations. Marcel Dekker AG, New York, pp 197–270

Brent RP (1973) Algorithms for minimization without derivatives. Prentice–Hall, Englewood Cliffs, chap 3–4

Bronaugh RL, Maibach HI (1985) Percutaneous absorption of nitroaromatic compounds: in vivo and in vitro studies in the human and monkey. J Invest Dermatol 84(3):180–183

Bronaugh RL, Stewart RF (1985) Methods for in vitro percutaneous absorption studies. iv: the flow–through diffusion cell. J Pharm Sci 74(1):64–67

Buist HE, van Burgsteden JA, Freidig AP, Maas WJM, van de Sandt JJM (2010) New in vitro dermal absorption database and the prediction of dermal absorption under finite conditions for risk assessment purposes. Regul Toxicol Pharmacol 57(2–3):200–209

Carslaw H, Jaeger J (1959) Conduction of heat in solids. Clarendon, Oxford, chap 128

Chatelain E, Gabard B, Surber C (2003) Skin penetration and sun protection factor of five uv filters: effect of the vehicle. Skin Pharmacol Appl Skin Physiol 16:28–35

Chen LJ, Lian GP, Han LJ (2007) Prediction of human skin permeability using artificial neural network (ANN) modeling. Acta Pharmacol Sin 28(4):591–600

Chien YW, Chien TY, Bagdon RE, Huang YC, Bierman RH (1989) Transdermal dual-controlled delivery of contraceptive drugs: formulation development, in vitro and in vivo evaluations, and clinical performance. Pharm Res 6:1000–1010

Cnubben NH, Elliott GR, Hakkert BC, Meuling WJ, van de Sandt JJ (2002) Comparative in vitro-in vivo percutaneous penetration of the fungicide ortho-phenylphenol. Regul Toxicol Pharmacol 35(2):198–208

Cooper ER, Berner B (1985) Finite dose pharmacokinetics of skin penetration. J Pharm Sci 74(10):1100–1102

Crank J (1975) The mathematics of diffusion, 2nd edn. Oxford University Press, London

Dancik Y, Anissimov YG, Jepps OG (2012) Convective transport of highly plasma protein bound drugs facilitates direct penetration into deep tissues after topical application. Br J Clin Pharmacol 73(4):564–578

Davies M, Pendlington RU, Page L, Roper CS, Sanders DJ, Bourner C, Pease CK, MacKay C (2011) Determining epidermal disposition kinetics for use in an integrated nonanimal approach to skin sensitization risk assessment. Toxicol Sci 119(2):308–318

Díez-Sales O, Copoví A, Casabó VG, Herráez H (1991) A modelistic approach showing the importance of the stagnant aqueous layers in in vitro diffusion studies, and in vitro–in vivo correlations. Int J Pharm 77(1):1–11

ECETOC (1993) Monograph 20, percutaneous absorption. European Centre for Ecotoxicology and Toxicology of Chemicals, Brussels

Elias PM (1983) Epidermal lipids, barrier function, and desquamation. J Invest Dermatol 80(Suppl):44s–49s

Escobar-Chavez JJ, Merino-Sanjuán V, López-Cervantes M, Urban-Morlan Z, Piñón Segundo E, Quintanar-Guerrero D, Ganem-Quintanar A (2008) The tape–stripping technique as a method for drug quantification in skin. J Pharm Pharm Sci 11(1):104–130

Feldmann RJ, Maibach HI (1969) Percutaneous penetration of steroids in man. J Invest Dermatol 52(1):89–94

Feldmann RJ, Maibach HI (1974) Percutaneous penetration of some pesticides and herbicides in man. Toxicol Appl Pharmacol 28(1):126–132

Fiserova-Bergerova V, Pierce JT, Droz PO (1990) Dermal absorption potential of industrial chemicals: criteria for skin notation. Am J Ind Med 17(5):617–635

Fisher HL, Most B, Hall LL (1985) Dermal absorption of pesticides calculated by deconvolution. J Appl Toxicol 5(3):163–177

Fitzpatrick D, Corish J, Hayes B (2004) Modelling skin permeability in risk assessment – the future. Chemosphere 55(10):1309–1314

Franz TJ, Lehman PA, Raney SG (2009) Use of excised human skin to assess the bioequivalence of topical products. Skin Pharmacol Physiol 22(5):276–286

Franz TJ (1975) Percutaneous absorption. On the relevance of in vitro data. J Invest Dermatol 64(3):190–195

Frasch F, Barbero AM (2013) Application of numerical methods for diffusion-based modeling of skin permeation. Adv Drug Deliv Rev 65(2):208–220

Frasch HF, Barbero AM (2008) The transient dermal exposure: theory and experimental examples using skin and silicone membranes. J Pharm Sci 97(4): 1578–1592

Frasch HF, Barbero AM, Hettick JM, Nitsche JM (2011) Tissue binding affects the kinetics of theophylline diffusion through the stratum corneum barrier layer of skin. J Pharm Sci 100(7):2989–2995

George K (2005) A two-dimensional mathematical model of non-linear dual-sorption of percutaneous drug absorption. Biomed Eng Online 4:40

Guy RH, Hadgraft J (1982) Percutaneous metabolism with saturable enzyme kinetics. Int J Pharm 11(3): 187–197

Guy RH, Hadgraft J (1985) Transdermal drug delivery: a simplified pharmacokinetic approach. Int J Pharm 24(2–3):267–274

Guy RH, Hadgraft J, Bucks DAW (1987) Transdermal drug delivery and cutaneous metabolism. Xenobiotica 17(3):325–343

Guy R, Hadgraft J, Maibach H (1982) A pharmacokinetic model for percutaneous absorption. Int J Pharm 11(2):119–129

Hadgraft J (1979) The epidermal reservoir; a theoretical approach. Int J Pharm 2(5–6):265–274

Hadgraft J (1980) Theoretical aspects of metabolism in the epidermis. Int J Pharm 4(3):229–239

Hahn T, Selzer D, Neumann D, Kostka KH, Lehr CM, Schaefer UF (2012) Influence of the application area on finite dose permeation in relation to drug type applied. Exp Dermatol 21(3):233–235

Hansen S, Henning A, Naegel A, Heisig M, Wittum G, Neumann D, Kostka KH, Zbytovska J, Lehr CM, Schaefer UF (2008) In–silico model of skin penetration based on experimentally determined input parameters. Part i: experimental determination of partition and diffusion coefficients. Eur J Pharm Biopharm 68(2):352–367

Hansen S, Naegel A, Heisig M, Wittum G, Neumann D, Kostka KH, Meiers P, Lehr CM, Schaefer U (2009)

The role of corneocytes in skin transport revised – a combined computational and experimental approach. Pharm Res 26:1379–1397

Hansen S, Lehr CM, Schaefer UF (2013) Improved input parameters for diffusion models of skin absorption. Adv Drug Deliv Rev 65(2):251–264

Heisig M, Lieckfeldt R, Wittum G, Mazurkevich G, Lee G (1996) Non steady–state descriptions of drug permeation through stratum corneum. i. The biphasic brick-and-mortar model. Pharm Res 13(3):421–426

Henning A, Schaefer UF, Neumann D (2009) Potential pitfalls in skin permeation experiments: influence of experimental factors and subsequent data evaluation. Eur J Pharm Biopharm 72(2):324–331

Herkenne C, Naik A, Kalia YN, Hadgraft J, Guy RH (2006) Ibuprofen transport into and through skin from topical formulations: in vitro–in vivo comparison. J Invest Dermatol 127(1):135–142

Herkenne C, Naik A, Kalia YN, Hadgraft J, Guy RH (2007) Dermatopharmacokinetic prediction of topical drug bioavailability in vivo. J Invest Dermatol 127(4):887–894

Herkenne C, Alberti I, Naik A, Kalia YN, Mathy FX, Préat V, Guy RH (2008) In vivo methods for the assessment of topical drug bioavailability. Pharm Res 25(1):87–103

Jones E, Oliphant T, Peterson P (2001) Scipy: open source scientific tools for python

Kasting GB (2001) Kinetics of finite dose absorption through skin 1. Vanillylnonanamide. J Pharm Sci 90(2):202–212

Krüse J, Golden D, Wilkinson S, Williams F, Kezic S, Corish J (2007) Analysis, interpretation, and extrapolation of dermal permeation data using diffusion–based mathematical models. J Pharm Sci 96(3):682–703

Kubota K, Koyama E, Twizell EH (1993) Dual sorption model for the nonlinear percutaneous kinetics of timolol. J Pharm Sci 82(12):1205–1208

Kubota K, Dey F, Matar SA, Twizell EH (2002) A repeated–dose model of percutaneous drug absorption. Appl Math Model 26(4):529–544

Kubota K (1991) A compartment model for percutaneous drug absorption. J Pharm Sci 80(5):502–504

Kurnik RT, Potts RO (1997) Modeling of diffusion and crystal dissolution in controlled release systems. J Control Release 45(3):257–264

Lademann J, Jacobi U, Surber C, Weigmann HJ, Fluhr JW (2009) The tape stripping procedure – evaluation of some critical parameters. Eur J Pharm Biopharm 72(2):317–323

Lehman PA, Raney SG, Franz TJ (2011) Percutaneous absorption in man: in vitro-in vivo correlation. Skin Pharmacol Physiol 24(4):224–230

Magnusson BM, Anissimov YG, Cross SE, Roberts MS (2004) Molecular size as the main determinant of solute maximum flux across the skin. J Invest Dermatol 122(4):993–999

McCarley KD, Bunge AL (2001) Pharmacokinetic models of dermal absorption. J Pharm Sci 90(11): 1699–1719

McCarley K, Bunge A (2000) Physiologically relevant two-compartment pharmacokinetic models for skin. J Pharm Sci 89(9):1212–1235

McKone TE, Howd RA (1992) Estimating dermal uptake of nonionic organic chemicals from water and soil: I. Unified fugacity–based models for risk assessments. Risk Anal 12(4):543–557

Melero A, Hahn T, Schaefer U, Schneider M (2011) In vitro human skin segmentation and drug concentration-skin depth profiles. In: Turksen K (ed) Permeability barrier, methods in molecular biology, vol 763. Humana Press, New York City, USA, pp 33–50

Michaels AS, Chandrasekaran SK, Shaw JE (1975) Drug permeation through human skin: theory and invitro experimental measurement. AIChE J 21(5):985–996

Muha I, Naegel A, Stichel S, Grillo A, Heisig M, Wittum G (2010) Effective diffusivity in membranes with tetrakaidekahedral cells and implications for the permeability of human stratum corneum. J Membr Sci 368(1–2):18–25

Naegel A, Hansen S, Neumann D, Lehr CM, Schaefer UF, Wittum G, Heisig M (2008) In–silico model of skin penetration based on experimentally determined input parameters. Part ii: mathematical modelling of in–vitro diffusion experiments. Identification of critical input parameters. Eur J Pharm Biopharm 68(2):368–379

Naegel A, Hahn T, Schaefer U, Lehr CM, Heisig M, Wittum G (2011) Finite dose skin penetration: a comparison of concentration–depth profiles from experiment and simulation. Comput Vis Sci 14(7):327–339

Naegel A, Heisig M, Wittum G (2013) Detailed modeling of skin penetration – an overview. Adv Drug Deliv Rev 65(2):191–207

Narkar Y (2010) Bioequivalence for topical products – an update. Pharm Res 27:2590–2601

Neumann D, Kohlbacher O, Merkwirth C, Lengauer T (2005) A fully computational model for predicting percutaneous drug absorption. J Chem Inf Model 46(1):424–429

Neumann D (2008) Modeling transdermal absorption. In: Ehrhardt C, Kim KJ (eds) Drug absorption studies, biotechnology: pharmaceutical aspects, vol VII. Springer, US, chap 20, pp 459–485

Nitsche JM, Frasch HF (2011) Dynamics of diffusion with reversible binding in microscopically heterogeneous membranes: general theory and applications to dermal penetration. Chem Eng Sci 66(10):2019–2041

OECD (2004a) Guidance document for the conduct of skin absorption studies. OECD Series on Testing and Assessment 28

OECD (2004b) Test guideline 428: skin absorption: in vitro method

Opdam JJG (1991) Linear systems dynamics in toxicokinetic studies. Ann Occup Hyg 35(6):633–649

Patel H, Berge W, Cronin MTD (2002) Quantitative structure-activity relationships (QSARs) for the prediction of skin permeation of exogenous chemicals. Chemosphere 48(6):603–613

Potts RO, Guy RH (1992) Predicting skin permeability. Pharm Res 9(5):663–669

Reddy MB, Guy RH, Bunge AL (2000a) Does epidermal turnover reduce percutaneous penetration? Pharm Res 17(11):1414–1419

Reddy M, McCarley K, Bunge A (2000b) Physiologically relevant one-compartment pharmacokinetic models for skin. 2. Comparison of models when combined with a systemic pharmacokinetic model. J Pharm Sci 87(4):482–490

Russell L, Guy R (2009) Measurement and prediction of the rate and extent of drug delivery into and through the skin. Expert Opin Drug Deliv 6(4):355–369

van de Sandt JJM, van Burgsteden JA, Cage S, Carmichael PL, Dick I, Kenyon S, Korinth G, Larese F, Limasset JC, Maas WJM, Montomoli L, Nielsen JB, Payan JP, Robinson E, Sartorelli P, Schaller KH, Wilkinson SC, Williams FM (2004) In vitro predictions of skin absorption of caffeine, testosterone, and benzoic acid: a multi–centre comparison study. Regul Toxicol Pharmacol 39(3):271–281

Schäfer-Korting M, Bock U, Diembeck W, Düsing HJ, Gamer A, Haltner-Ukomadu E, Hoffmann C, Kaca M, Kamp H, Kersen S, Kietzmann M, Korting HC, Krächter HU, Lehr CM, Liebsch M, Mehling A, Müller-Goymann C, Netzlaff F, Niedorf F, Rübbelke MK, Schaefer U, Schmidt E, Schreiber S, Spielmann H, Vuia A, Weimer M (2008) The use of reconstructed human epidermis for skin absorption testing: results of the validation study. ATLA Altern Lab Anim 36(2): 161–187

Scheuplein RJ, Ross LW (1974) Mechanism of percutaneous absorption. v. Percutaneous absorption of solvent deposited solids. J Invest Dermatol 62(4):353–360

Scheuplein RJ (1967) Mechanism of percutaneous absorption. ii. Transient diffusion and the relative importance of various routes of skin penetration. J Invest Dermatol 48(1):79–88

Selzer D, Abdel-Mottaleb M, Hahn T, Schaefer UF, Neumann D (2013a) Finite and infinite dosing: difficulties in measurements, evaluations and predictions. Adv Drug Deliv Rev 65(2):278–294

Selzer D, Hahn T, Naegel A, Heisig M, Kostka KH, Lehr CM, Neumann D, Schaefer UF, Wittum G (2013b) Finite dose skin mass balance including the lateral part: comparison between experiment, pharmacokinetic modeling and diffusion models. J Control Release 165(2):119–128

Seta Y, Ghanem AH, Higuchi WI, Borsadia S, Behl CR, Malick AW (1992) Physical model approach to understanding finite dose transport and uptake of hydrocortisone in hairless guinea–pig skin. Int J Pharm 81(1):89–99

Shah VP, Flynn GL, Yacobi A, Maibach HI, Bon C, Fleischer NM, Franz TJ, Kaplan SA, Kawamoto J, Lesko LJ, Marty JP, Pershing LK, Schaefer H, Sequeira JA, Shrivastava SP, Wilkin J, Williams RL (1998) AAPS/FDA Workshop report: bioequivalence of topical dermatological dosage forms: methods of evaluation of bioequivalence, vol 22. Advanstar Communications, Duluth

Simon L, Goyal A (2009) Dynamics and control of percutaneous drug absorption in the presence of epidermal turnover. J Pharm Sci 98(1):187–204

Sloan KB, Wasdo SC, Rautio J (2006) Design for optimized topical delivery: prodrugs and a paradigm change. Pharm Res 23(12):2729–2747

Stinchcomb AL, Pirot F, Touraille GD, Bunge AL (1999) Chemical uptake into human stratum corneum in vivo from volatile and non–volatile solvents. Pharm Res 16(8):1288–1293

Talreja PS, Kasting GB, Kleene NK, Pickens WL, Wang TF (2001) Visualization of the lipid barrier and measurement of lipid pathlength in human stratum corneum. AAPS PharmSci 3(2):48–56

Treffel P, Gabard B (1996) Skin penetration and sun protection factor of ultra-violet filters from two vehicles. Pharm Res 13:770–774

Vaughan DP, Dennis M (1978) Mathematical basis of point-area deconvolution method for determining in vivo input functions. J Pharm Sci 67(5):663–665

Wagner H, Kostka KH, Lehr CM, Schaefer UF (2000) Drug distribution in human skin using two different in vitro test systems: comparison with in vivo data. Pharm Res 17(12):1475–1481

Wagner H, Kostka KH, Lehr CM, Schaefer UF (2002) Human skin penetration of flufenamic acid: in vivo/in vitro correlation (deeper skin layers) for skin samples from the same subject. J Invest Dermatol 118(3):540–544

Wallace SM, Barnett G (1978) Pharmacokinetic analysis of percutaneous absorption: evidence of parallel penetration pathways for methotrexate. J Pharmacokinet Biopharm 6(4):315–325

Wearley LL, Tojo K, Chien YW (1990) A numerical approach to study the effect of binding on the lontophoretic transport of a series of amino acids. J Pharm Sci 79(11):992–998

Wester RC, Maibach HI (1976) Relationship of topical dose and percutaneous absorption in rhesus monkey and man. J Invest Dermatol 67(4):518–520

Wilkinson SC, Maas WJM, Nielsen JB, Greaves LC, Sandt JJM, Williams FM (2006) Interactions of skin thickness and physicochemical properties of test compounds in percutaneous penetration studies. Int Arch Occup Environ Health 79(5):405–413

Wilschut A, ten Berge WF, Robinson PJ, McKone TE (1995) Estimating skin permeation. The validation of five mathematical skin permeation models. Chemosphere 30(7):1275–1296

Zhang Q, Li P, Roberts MS (2011) Maximum transepidermal flux for similar size phenolic compounds is enhanced by solvent uptake into the skin. J Control Release 154(1):50–57